Journal Pre-proof

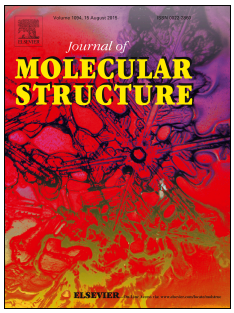

Synthesis, characterization, *in silico* studies and *in vitro* biological evaluation of isoniazid-hydrazone complexes

M.P. Ramya Rajan, Rathikha Ramaswamy, Nithyabalaji Rajendran, Sribalan Rajendran

PII: S0022-2860(20)30622-0

DOI: https://doi.org/10.1016/j.molstruc.2020.128297

Reference: MOLSTR 128297

To appear in: *Journal of Molecular Structure*

Received Date: 21 December 2019

Revised Date: 26 March 2020

Accepted Date: 17 April 2020

Please cite this article as: M.P.R. Rajan, R. Ramaswamy, N. Rajendran, S. Rajendran, Synthesis, characterization, *in silico* studies and *in vitro* biological evaluation of isoniazid-hydrazone complexes, *Journal of Molecular Structure* (2020), doi: https://doi.org/10.1016/j.molstruc.2020.128297.

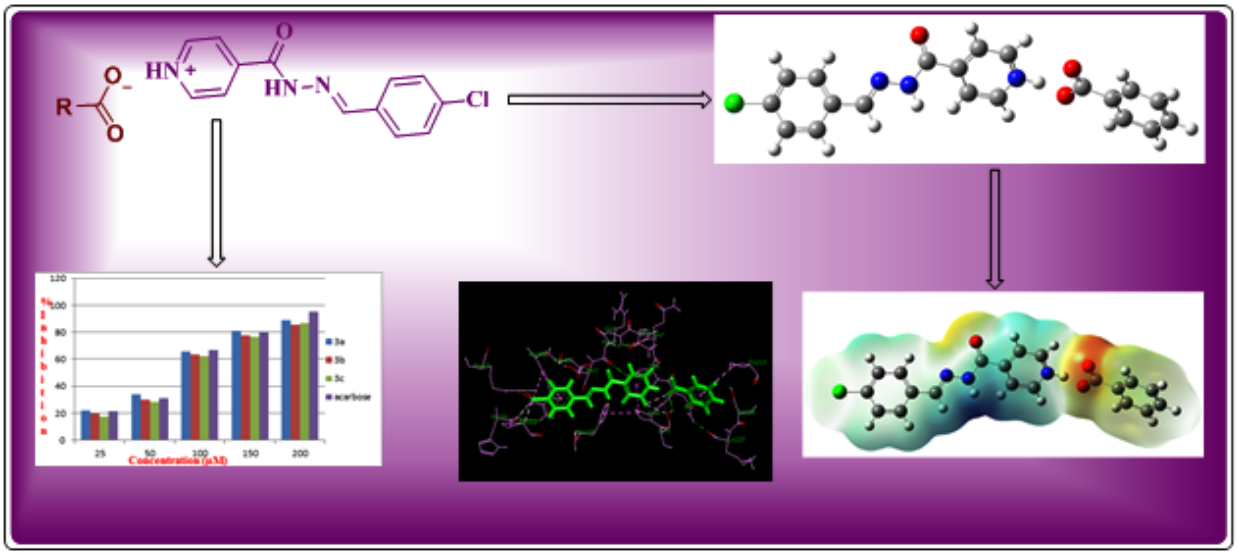

Table 1: DFT calculations of IHCs .

S. No	Compound name	HOMO (eV)	LUMO (eV)	Band gap(ΔE) (eV)	Chemical potential (eV)	Global hardness (eV)	Global softness (eV^{-1})	Electrophillicity index (eV)
1.	3a	-5.7811	-3.2787	2.5024	-4.5299	1.2512	0.3996	8.2003
2	3b	-6.0182	-3.2765	2.7416	-4.6474	1.3708	0.3647	7.8779
3	3c	-5.5670	-3.3971	2.1698	-4.4820	1.0849	0.4608	9.2581

Table 2: Molecular docking interaction of IHCs against α-amylase.

S. No	Compound Name	1HNY		
		Binding energy (KJ/mol)	No. of hydrogen bonding	Hydrogen bonded amino acid residue
1	3a	-294.42	2	SER3, ARG421
2	3b	-315.83	2	SER3, TYR2
3	3c	-299.78	5	THR377, TRP388, ARG389, GLN390,LYS322

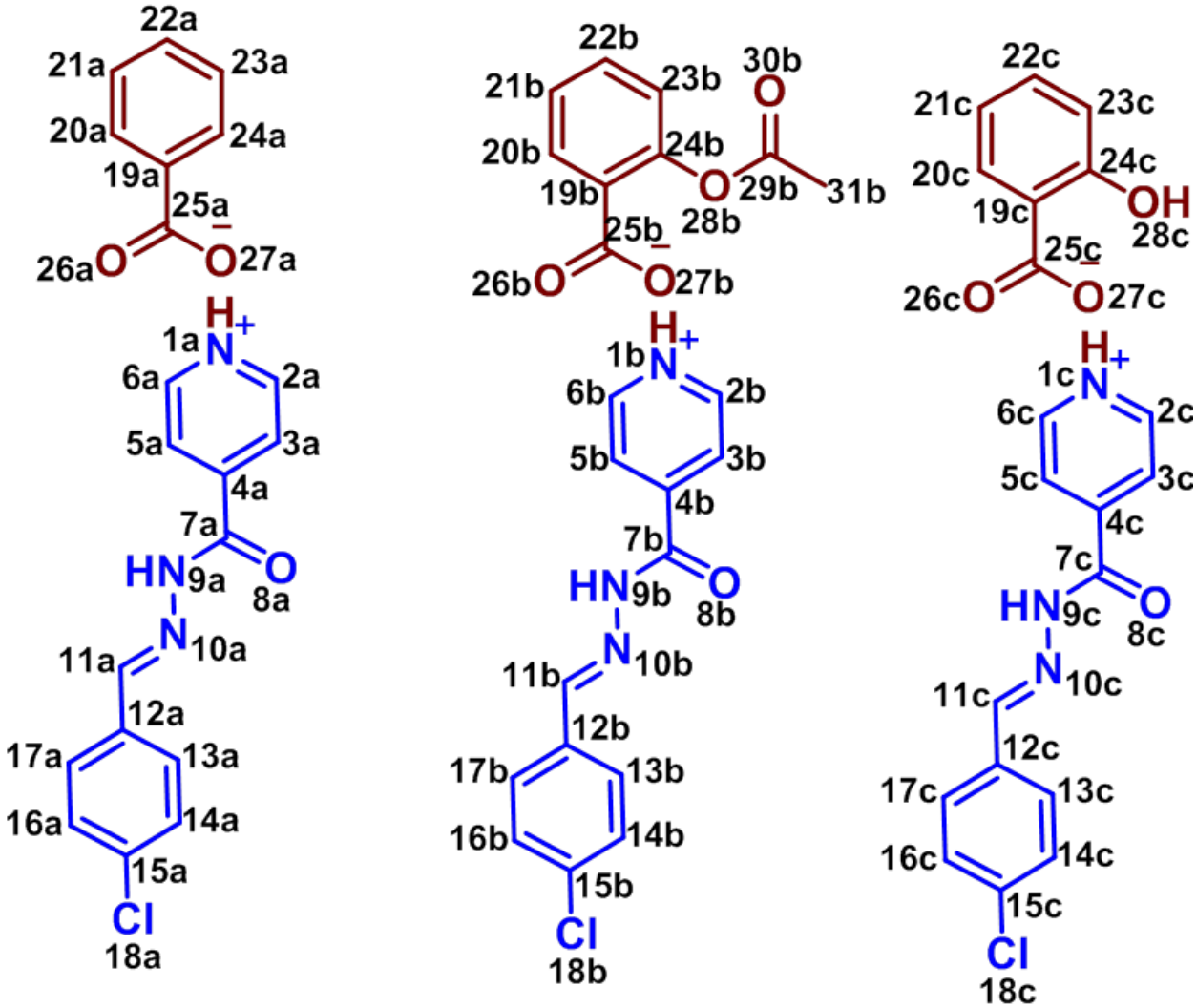
22a
21a
23a
20a
24a
19a
25a
26a
O
O
27a
H
1a
N+
6a
2a
5a
3a
4a
7a
HN
9a
O
8a
N
10a
11a
12a
17a
13a
16a
14a
15a
Cl
18a
22b
21b
23b
30b
O
20b
24b
19b
O
29b
31b
28b
25b
26b
O
O
27b
H
1b
N+
6b
2b
5b
3b
4b
7b
HN
9b
O
8b
N
10b
11b
12b
17b
13b
16b
14b
15b
Cl
18b
22c
21c
23c
20c
24c
19c
OH
28c
25c
26c
O
O
27c
H
1c
N+
6c
2c
5c
3c
4c
7c
HN
9c
O
8c
N
10c
11c
12c
17c
13c
16c
14c
15c
Cl
18c

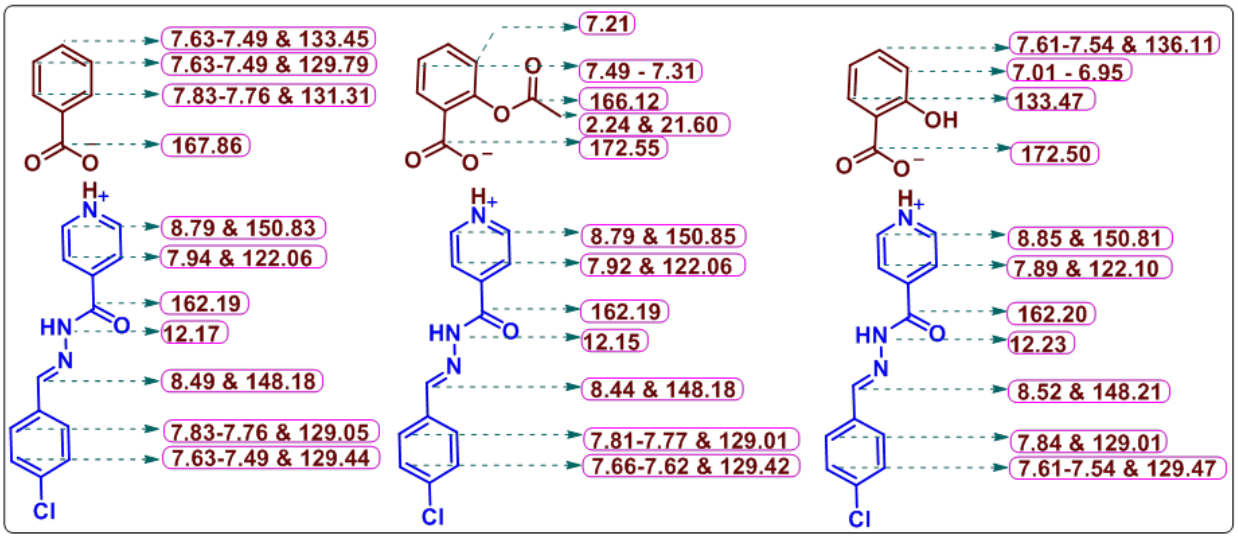

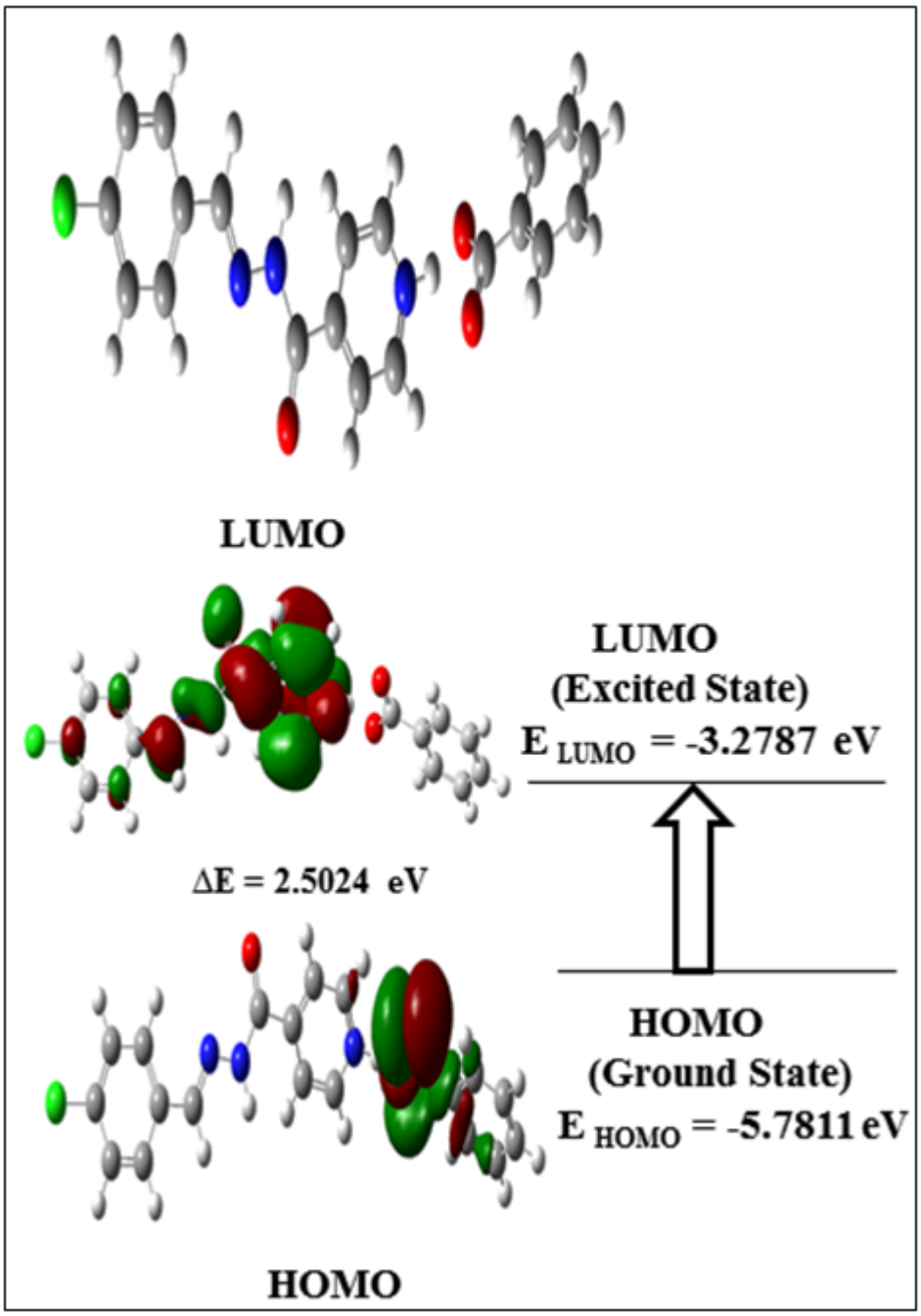
LUMO
LUMO
(Excited State)
E LUMO = -3.2787 eV
ΔE = 2.5024 eV
HOMO
(Ground State)
E HOMO = -5.7811 eV
HOMO

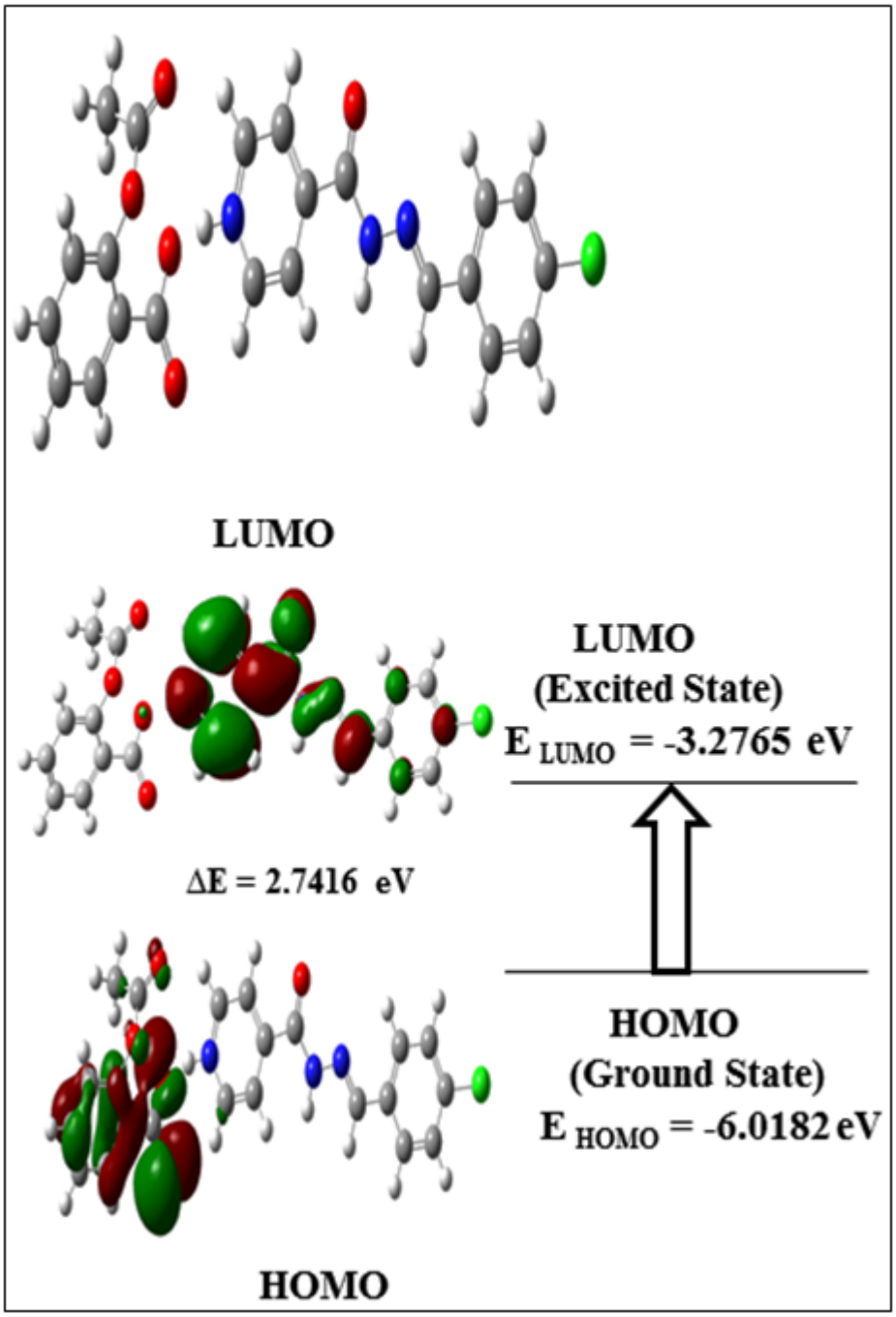
LUMO
LUMO
(Excited State)
E LUMO = -3.2765 eV
ΔE = 2.7416 eV
HOMO
(Ground State)
E HOMO = -6.0182 eV
HOMO

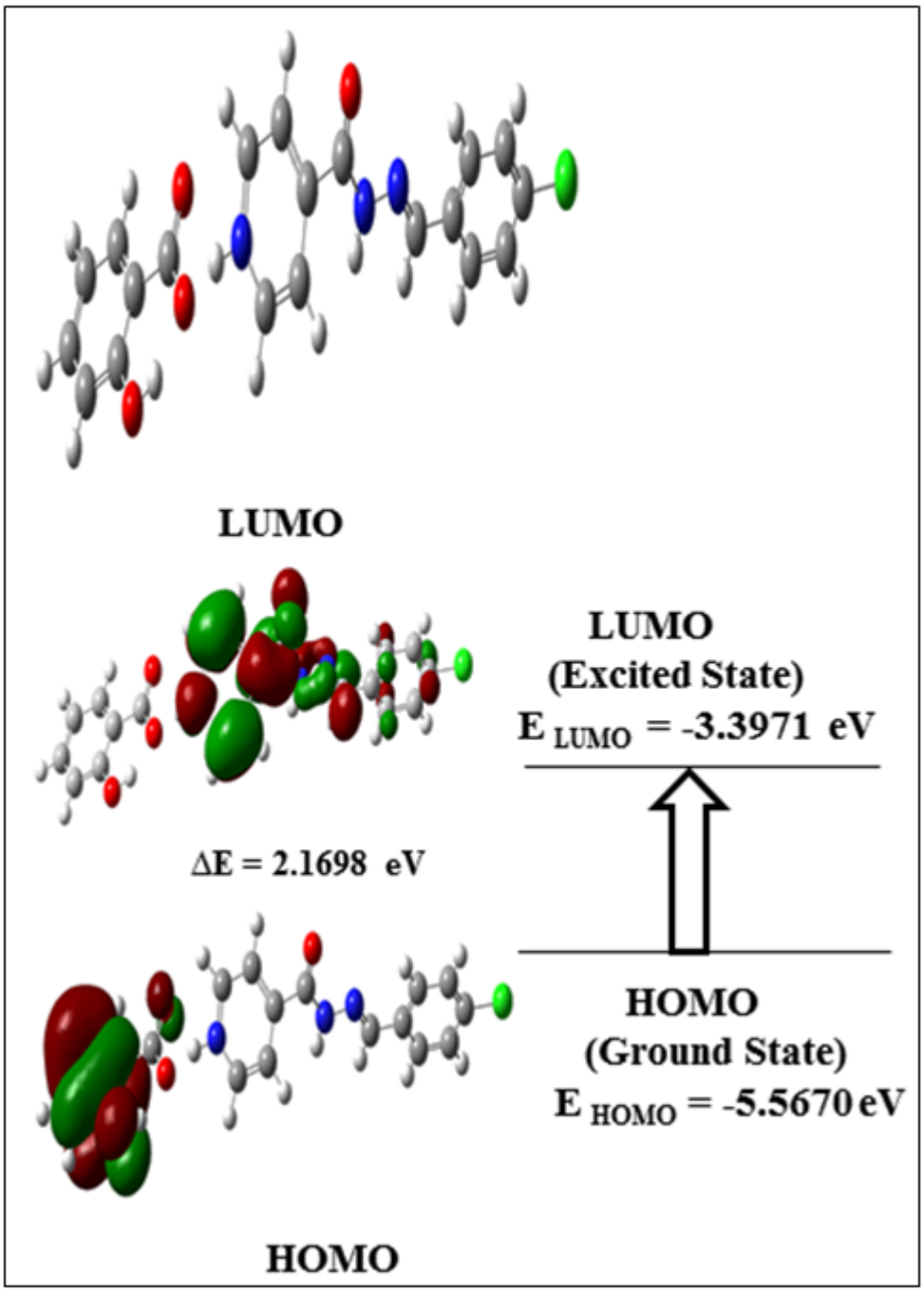
LUMO
LUMO
(Excited State)
E LUMO = -3.3971 eV
ΔE = 2.1698 eV
HOMO
(Ground State)
E HOMO = -5.5670 eV
HOMO

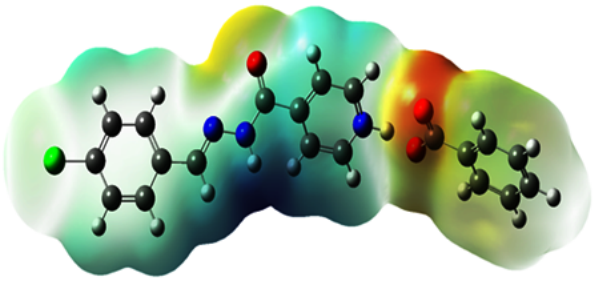

Molecular electrostatic potential of compound 3a

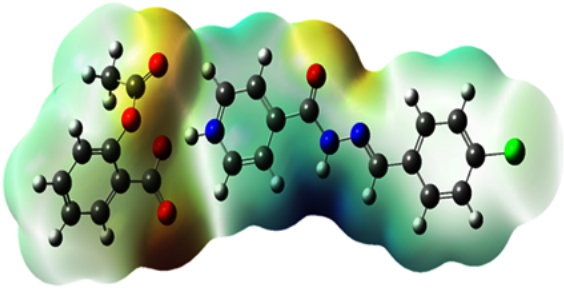

Molecular Electrostatic potential of compound 3b

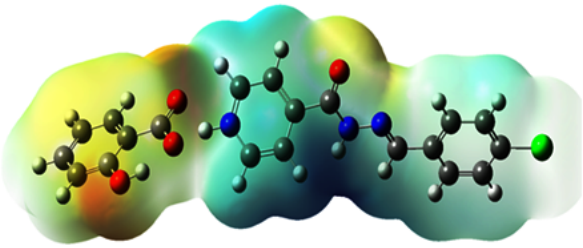

Molecular Electrostatic potential of compound 3c

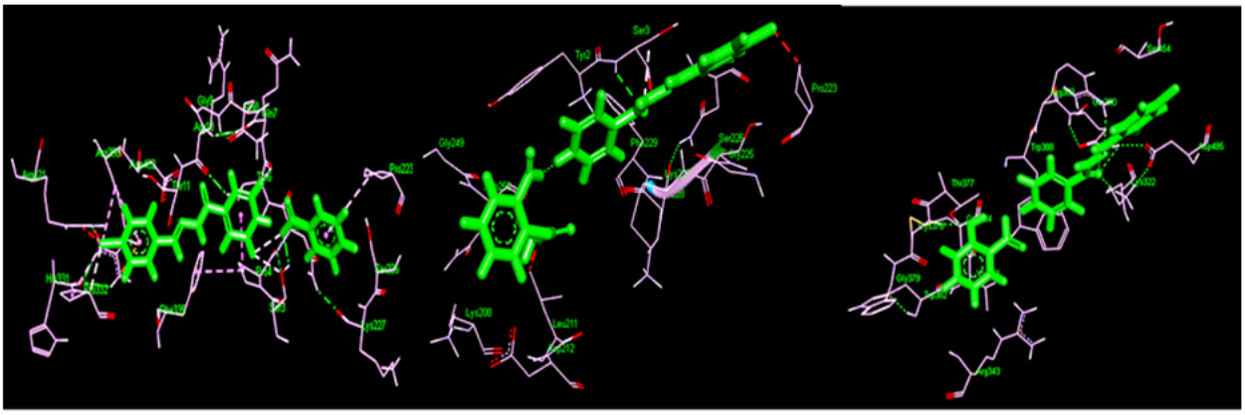

Interaction of compound 3a with 1HNY

Interaction of compound 3b with 1HNY

Interaction of compound 3c with 1HNY

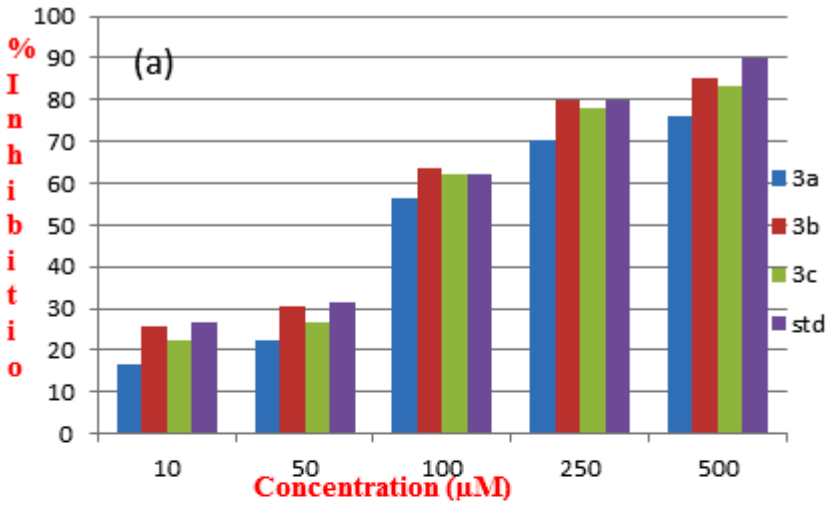
(a)
% Inhibition
100
90
80
70
60
50
40
30
20
10
0
10
50
100
250
500
Concentration (µM)
3a
3b
3c
std

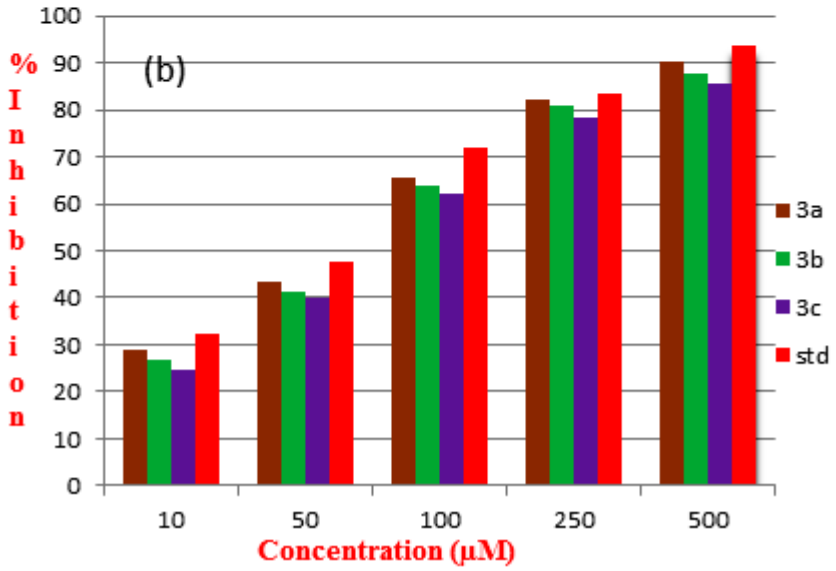
(b)
% Inhibition
100
90
80
70
60
50
40
30
20
10
0
10
50
100
250
500
Concentration (µM)
3a
3b
3c
std

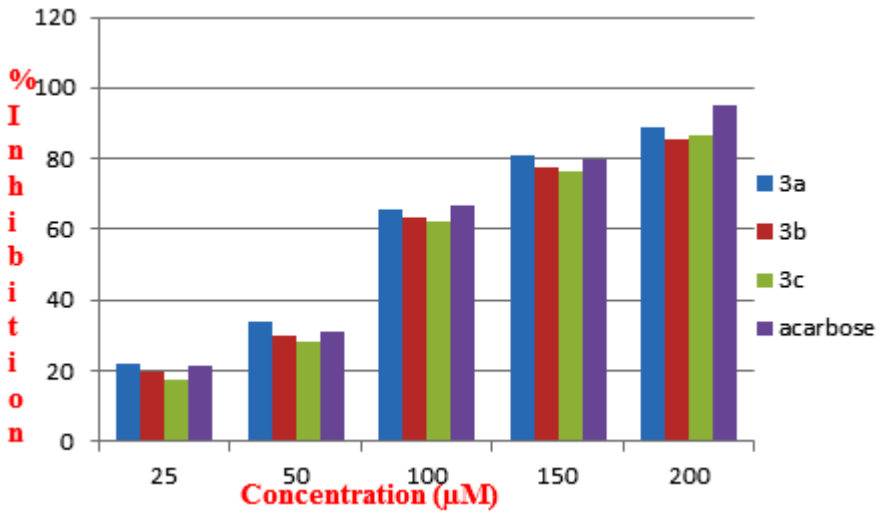

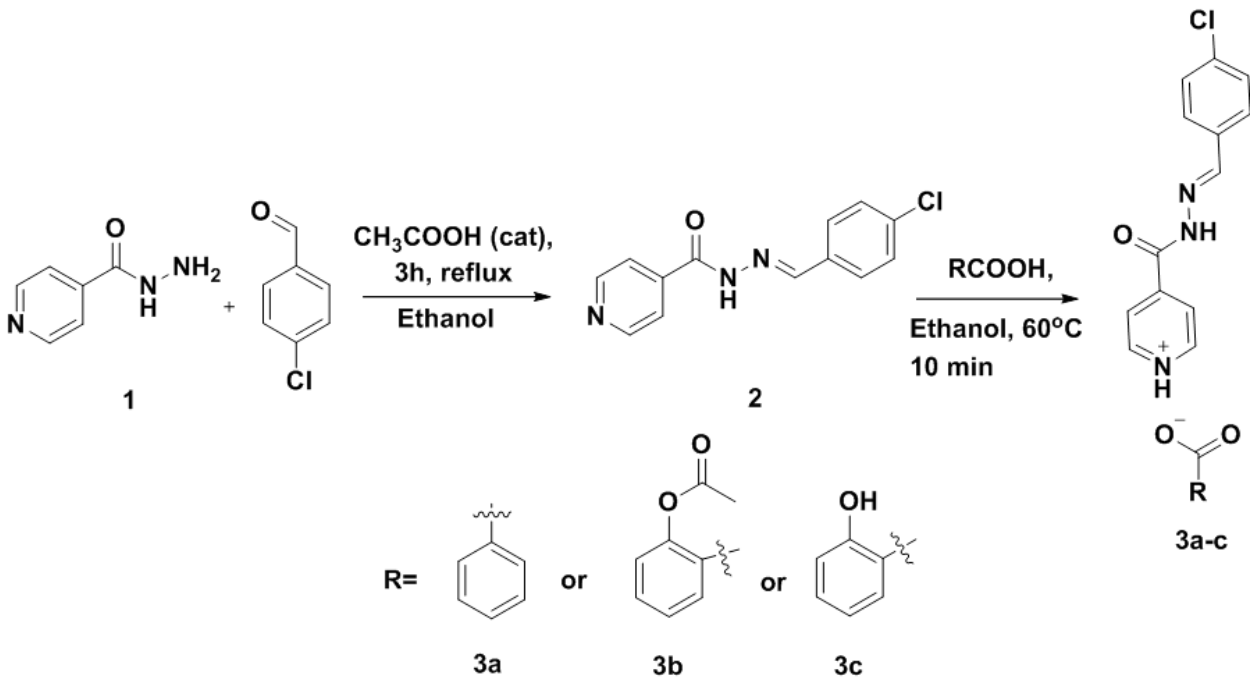
CH3COOH (cat),
3h, reflux
Ethanol
RCOOH,
Ethanol, 60°C
10 min
1
2
3a-c
R=
or
or
3a
3b
3c

- The synthesis of IHCs is economically cheaper and simple method.
- The IHCs proved as anti-inflammatory and antidiabetic agents at *in vitro* level.
- Hydrazone-salicylate complex forms 5 hydrogen bonding interaction with 1HNY.
- Electrophilicity index of hydrazone-salicylate complex is higher than others.
- FMO studies showed the electron cloud localized in the benzoate and pyridinium.

Author contributions

Mrs. Ramya Rajan M.P.	: Synthesis and characterization of IHCs and Molecular docking.
Dr. Ramaswamy Rathikha	: Research work design and scientific discussions.
Mrs. Rajendran Nithyabalaji	: DFT studies.
Dr. Rajendran Sribalan	: Testing and analysis (*in vitro* biological studies).

Declaration of interests

☒ The authors declare that they have no known competing financial interests or personal relationships that could have appeared to influence the work reported in this paper.

☐The authors declare the following financial interests/personal relationships which may be considered as potential competing interests:

The authors declare that they have no known competing financial interests or personal relationships that could have appeared to influence the work reported in this paper.

Synthesis, characterization,*insilico*studies and *invitro* biological evaluation of Isoniazid-hydrazone complexes

RamyaRajanM.P,[a*]RamaswamyRathikha,[b]RajendranNithyabalaji,[a]RajendranSribalan[c]

[a]*Department of Physics, SRM Valliammai Engineering College, Kattankulathur, Chengalpet Dt., Tamil Nadu, India*

[b]*Department of Physics,Presidency College, Chennai, Tamil Nadu, India*

[c]*Biochemie Innovations Lab, Tindivanam, Tamil Nadu, India.*

Corresponding author e-mail:ramyarajanmp@gmail.com***

Abstract

Isoniazid-hydrazonecomplexes (IHCs)were synthesized and thoroughly characterized by FT-IR, ^{1}H NMR and ^{13}C NMRspectroscopic techniques. The anti-inflammatory and antidiabetic activities were tested for the IHCs using protein denaturation methods and the α-amylase inhibitory method. The molecular modeling studies for IHCswere investigated and their molecular parameters were calculated using Density Functional Theory methods. The IHCs showed lower band gap and higher electrophilicity index values. Further, molecular docking studies were investigated against the α-amylase enzyme to compare the experimental results. The isoniazidhydrazone-salicylic acid complex (3c) showed five hydrogen bonding interactions with aminoacid residues of the α-amylase enzyme (1HNY).

Keywords: Isoniazid, Anti-inflammatory, Antidiabetic, Molecular docking, DFT studies.

1. Introduction

Isoniazid is primarily used anti-tuberculosis drug [1] as well as antimicrobial drug, which is an isomer of nicotinic hydrazide [2].The side effect of isoniazid is the elevation of liver enzymes level in blood and hepatic toxicity appears as cellular necrosis, steatosis [3]. Metabolites of this drug also have toxic effects on liver cells [4].Hydrazine is one of the most

important metabolites of isoniazid [5].The derivatives of isoniazid may overcome these problems.The hydrazones are simple derivatives of hydrazines. Moreover, hydrazones possess a wide range of pharmacological activities such as antimicrobial [6], anticonvulsant [7],analgesics [8], anti-inflammatory [9], antitubercular [10] and antitumor [11] activities. For instance, isoniazid hydrazones are antitubercular agents [12] and alsothe incorporation of hydrazoneunit in isoniazid maintaining antimycobacterial activity. Therefore hydrazones of isoniazid, retaining its activity, avoid toxicity and it showed better effectiveness than isoniazid [13].

The combinations of drug molecules can help to improve therapeutic efficiency than single agents[14]. Nowadays the drug combination therapy is a promising strategy for multiple complex diseases [15]. Some of thesecombinations were found to be impressive because which is reducing the toxicity and side effects. For example, both glyburide and metformin are used for the treatment of type 2 diabetes. The glyburide reduces insulin resistance and metformin increases insulin secretion respectively. In this combination of two drug molecules, therapeutic efficacy improves due to their complementary mechanism [16-17]. The physical and chemical properties of complexes are completely varied from the parent drugs. It is an important process in drug discovery research because the complexation improves the solubility and stability of the drug[18]. For example, the complex of theophylline with ethylenediamine (aminophylline) has very good stability[19]. Similarly, the cyclodextrincomplexation process was used to improve the stabilityin many drug developments[20].

Based on the above knowledge, the isoniazid hydrazone is focused onthe synthesis and characterized. The isoniazid-hydrazones (IHCs) are planning for complexation with three bioactive compounds like benzoic acid, aspirin and salicylic acid **(Fig. 1)**. The complete

*invitro*experimental and *insilico* studies were performed to investigate the biological importance of IHCs.

2. Experimental section

2.1 Materials and methods

The analytical grade solvents were usedand purchasedfrom SpectrochemorSigma Aldrich. Reactions were monitored by the TLC platewhich is on precoated silica gel 60 F254 in TLC sheets (0.2mm thickness, Merck plate) and 60-120 mesh Merck silica gel used for column chromatography. Petroleum ether and ethyl acetate wereused as the eluents. ^{1}H and ^{13}C NMR spectra were recorded on Bruker 300 MHz and 75 MHz instruments, $CDCl_3$and DMSO-$d_6$were used as an internal solvent. Chemical shift values were represented in δ (ppm) and coupling constants are mentioned in terms of Hz with the internal reference TMS. ESI-MS spectra were recorded in the LCQ fleet mass spectrometer. FT-IR spectra were recorded in Thermo Scientific Nicolet iS50 FT-IR Spectrometer.

2.2 Synthetic procedure for (E)-N'-(4-chlorobenzylidene)isonicotinohydrazide (2)

The isonicotinic hydrazide (3.0 g, 21.89 mmol) and *p*-chlorobenzaldehye (3.06 g, 21.89) were dissolved in ethanol (30 mL). To that solution glacial acetic acid (0.1 mL) was added. The reaction mixture was refluxed for 3 hours at 80 °C. Then the reaction mixture was cooled to room temperature. The obtained solid was filtered washed with cooled ethanol (5mL).

White solid.^{1}H NMR (300 MHz, DMSO-d_6+$CDCl_3$) δ 8.73 (d, *J* = 5.4 Hz, 2H), 8.42 (s, 1H), 7.81 (d, *J* = 5.1 Hz, 2H), 7.74 (d, *J* = 7.5 Hz, 2H), 7.37 (d, *J* = 7.2 Hz, 2H).^{13}C NMR (75 MHz, $CDCl_3$) δ 161.23, 148.96, 147.24, 139.40, 134.56, 131.51, 127.74, 127.63, 120.52.ESI-MS calculated 259.05 found 260 $[M+1]^+$.IR (KBr Disc) cm^{-1}:3164.20, 1659.39, 1596.83, 1551.06, 816.46.

2.3 Preparation of 3a-c

The intermediate **2** (10 mmol) and corresponding carboxylic acid (10 mmol) was dissolved in ethanol (10 mL) and heated for 10 min and cooled to room temperature. The evaporation of the solvent yielded target compounds.

2.3.1(E)-4-(2-(4-chlorobenzylidene)hydrazine-1-carbonyl)pyridin-1-ium benzoate (3a)

White solid.^{1}H NMR (300 MHz, DMSO-d_6) δ 12.17 (s, 1H), 8.78(d, *J* = 4.8 Hz, 2H), 8.49 (bs, 1H), 7.94 (d, *J* = 7.2 Hz, 2H), 7.83-7.76 (m, 4H), 7.63 – 7.49 (m, 5H).^{13}C NMR (75 MHz, DMSO-d_6) δ 167.86, 162.19, 150.83, 150.07, 148.18, 140.85, 135.37, 133.45, 133.34, 131.31, 129.79, 129.44, 129.05, 122.06.IR (KBr Disc) cm^{-1}: 3027.86, 1738.39, 1661.95, 1560.18, 847.46.706.71.

2.3.2 (E)-4-(2-(4-chlorobenzylidene)hydrazine-1-carbonyl)pyridin-1-ium 2-acetoxybenzoate (3b)

White solid.^{1}H NMR (300 MHz, DMSO-d_6) δ 12.15 (s, 1H), 8.79 (d, *J* = 4.8 Hz, 2H), 8.44 (s, 1H), 7.92 (br s, 2H), 7.81-7.77 (m, 3H), 7.66-7.62 (m, 2H), 7.54 (br s, 1H), 7.40 – 7.36 (m, 1H), 7.21 (brs, 1H), 2.24 (s, 3H).^{13}C NMR (75 MHz, DMSO-d_6) δ 172.55, 169.71, 166.12, 162.19, 150.85, 148.18, 140.87, 135.37, 134.32, 133.48, 131.90, 129.42, 129.01, 126.58, 124.54, 124.29, 122.06, 21.60.IR (KBr Disc) cm^{-1}:3025.83, 1748.96, 1662.10, 1604.57, 1293.55, 851.62, 752.78.

2.3.3(E)-4-(2-(4-chlorobenzylidene)hydrazine-1-carbonyl)pyridin-1-ium 2-hydroxybenzoate (3c)

White solid.^{1}H NMR (300 MHz, DMSO-d_6) δ 12.23 (s, 1H), 8.85 (d, *J* = 4.8 Hz, 2H), 8.52 (s, 1H), 7.89 (d, *J* = 5.1 Hz, 2H), 7.88-7.85 (m, 3H), 7.61-7.54 (d, *J* = 8.1 Hz, 3H), 7.01-6.95 (m, 2H). ^{13}C NMR (75 MHz, DMSO-d_6) δ 172.50, 162.20, 161.70, 150.81, 148.21, 140.92, 136.11, 135.39, 133.47, 130.80, 129.47, 129.01, 127.46, 122.10, 119.67, 117.61, 113.51. IR (KBr Disc) cm^{-1}: 3027.36, 1738.45, 1659.56, 1591.85, 1216.91, 849.56, 751.88.

2.4 Anti-inflammatory activity

2.4.1 Protein denaturation technique

The IHCs were tested for anti-inflammatory activity using the inhibition of albumin denaturation technique followed by the literature reports [21-23].

2.5 Antidiabetic Activity

2.5.1*α*- amylase inhibitory activity

The *α*-amylase inhibitory activity was carried out by following the reported literature [24].

2.6 Molecular docking study

The molecular docking studies were performed followed by the reported literature method [25]. Molecular docking of compounds was carried out with crystal structures of 1HNY and performed using the Hex 8.0 software. The three dimensional structure of IHCswas constructed usingChemBio 3D ultra 13.0 software and then they were energetically minimized using MMFF94 with the maximum number of iteration of 5000 andminimum RMS gradient of 0.10 [26]. The crystal structure of the protein was taken from Protein Data bank (www.rcsb.org) and chain A was selected for docking studies. All bound water and ligand were eliminated from

the protein and polar hydrogen was added to the protein as it is required for the electrostatics and then nonpolar hydrogen atoms were merged. The ligand was docked in the active site of 1HNY [27]. The docking parameters were used as default in Hex 8.0.

2.7 Computational calculations

All the computational calculations including representation of Highest occupied molecular orbital (HOMO) and lowest unoccupied molecular orbital (LUMO) in the checkpoint files were performed with the Gaussian 09W program using density functional theory [28]. The chemical structure of the IHCs was optimized with B3LYP/6.311 ++ G(d,p) basis set. The Gauss view software package was used to visualize the computed structures including HOMO, LUMO and Molecular electrostatic potential (MEP) representations.

3. Results and Discussions

3.1 Chemistry

The reaction of isoniazid with *p*-chlorobenzaldehyde at reflux condition yielded the required starting material **2**.The complexation of **2** with corresponding carboxylic acids yielded various IHCs. The overall synthetic route for IHCs was represented in **Scheme 1**.

3.1.1 Characterization

3.1.1.1 Compound 3a

The ^{1}H NMR clearly showed that the compound 3a contains 14 numbers of protons (the pyridinium proton is a labile proton, which may not appear in the spectrum). The appearance singlet at 12.17 ppm for one proton indicates the presence of a hydrazide NH unit. The sharp singlet for one proton at 8.49 ppm has appeared for the imine CH unit. The doublet at 8.79 ppm for 2 protons appeared for 2a & 6a protons of pyridinium unit. Similarly, the doublet at 7.94 ppm for 2 protons appeared for 3a & 5a protons of pyridinium unit. The signals around 7.83-7.76 ppm appeared for 13a & 17a protons of the *p*-chlorophenylene unit. Similarly, the signals around

7.63-7.49 ppm appeared for 14a & 16a protons of the *p*-chlorophenylene unit. Another protons signals around 7.63-7.49 & 7.83-7.76 ppm appeared for the benzoate unit.

The ^{13}C NMR showed that the compound 3a contains 14 sets of carbon signals. The appearance of the carbon signal at 167.86 ppm indicates the presence of carboxylate carbon and the peak appeared at 162.19 ppm indicates the presence of hydrazide carbon. The appearance of a peak at 148.18 ppm has appeared for imine carbon. The carbon signal at 150.83 ppm has appeared for 2a and 6a carbons for the pyridinium unit. Similarly, 3a and 5a carbons of pyridinium unit appeared at 122.06 ppm respectively. The *p*-chlorophenylene carbons 13a & 17a appeared at 129.05 and 14a & 16a carbons appeared at 129.44 ppm respectively. The benzoate phenyl carbons like 20a-24a appeared in the region of 130.11 to 131.63 ppm correspondingly.

The FT-IR spectrum gave some additional evidence for compound formations. The appearance of the medium absorption band at 3460 cm^{-1} indicates the presence of a hydrazide NH unit. Similarly, the appearance of the medium absorption band at 3400 cm^{-1} indicates the presence of the pyridinium NH unit. The stretching frequencies at 3029 and 2970 cm^{-1} indicate the presence of aromatic rings which appeared for the stretching frequency of aromatic CH units. The strong absorbance at 1738 cm^{-1}indicates the presence of carboxylate and hydrazide carbonyl units. The imine stretching frequency has appeared at 1661 cm^{-1}.The stretching frequency for the C=N unit of pyridiniumhas appeared at 1591 cm^{-1} and the stretching frequency of C=C for aromatic rings appeared at 1560 cm^{-1}. The stretching frequency around 1215 cm^{-1} indicates the presence of the C-O unit which is present in the carboxylate of benzoate moiety. The C-Cl stretching frequency has appeared at 707 cm^{-1}.

3.1.1.2 Compound 3b

The compound 3b has 16 numbers of protons, the ^{1}H NMR spectrum of 3b clearly showed proton signals for 15 protons (the pyridiniumNH is a labile proton, which may not appear in the spectrum). The appearance of a doublet at 8.79 ppm for 2 protons and the appearance of a signal at 7.94 ppm for 2 protons indicate the presence of a pyridinium unit. These signals have appeared for 2b, 6b, 3b and 5b protons of pyridinium unit correspondingly. The singlets at 8.44 ppm and 12.15 ppm appeared for hydrazide and imine unit respectively. The proton signals for 13a & 17a in the region of 7.81-7.77 ppm and 14a & 16a protons appeared at 7.66-7.62 ppm correspondingly which belongs to the *p*-chlorophenylene unit. The sharp singlet for 3 protons at 2.24 ppm appeared for acetate CH_3 unit. The signals around 7.49-7.31& 7.21 ppm appeared for aspirin phenylene protons.

Similarly, the compound 3b contains 18 sets of carbon signals, the ^{13}C NMR spectrum also showed 18 sets of carbon signals. The peak at 172.55 ppm appeared for the carboxylate unit of aspirin. The carbon signal at 166.12 ppm appeared for acetate carbon of the aspirin unit. The appearance of the carbon signal at 162.19 ppm indicates the presence of hydrazide which is present in the pyridinium hydrazide unit. The carbon signal at 148.18 ppm appeared for the imine unit. The appearance of carbon signals at 150.85 & 122.06 ppm indicates the presence of pyridinium unit which belongs to 2b, 6b, 3b and 5b carbons. The appearance of carbon signals at 129.01 & 129.42 ppm indicates the presence of the *p*-chlorophenylene unit.

In the FT-IR spectrum, the medium absorption band at 3490 cm^{-1} indicates the presence of hydrazide stretching frequency. Similarly, the appearance of stretching frequency at 3400 cm^{-1} indicates the presence of the pyridinium NH unit. The absorption band at 3075, 3026 and 2846 cm^{-1} is appeared for aromatic CH stretching vibrations. The absorption band at 1746 cm^{-1}has

appeared for hydrazide carbonyl and carboxylate carbonyl units. The strong absorption band at 1660 cm^{-1}has appeared for the C=N stretching vibration of imine moiety. The band at 1603 cm^{-1} and 1560 cm^{-1}appeared for the C=NH unit of pyridinium and C=C unit of aromatic rings. The band at 1293 and 1216 cm^{-1} appeared for C-O stretching vibrations of carboxylate units. The C-Cl stretching vibration appeared at 751 cm^{-1} as a strong absorption band.

3.1.1.3 Compound 3c

The compound 3c contains 16 numbers of protons, the ^{1}H NMR spectrum showed the signals for 14 protons (the phenolic proton and pyridinium protons are labile protons which may not appear in the spectrum). The singlets at 12.23 and 8.52 ppm indicate the presence of hydrazide NH and imine CH units. The proton signal at 8.85 ppm for 2 protons appeared for 2c & 6c protons of pyridinium unit. Similarly, the appearance of the proton signal at 7.89 ppm for 2 protons appeared for 3c & 5c protons of pyridinium unit. The appearance of protons signals at 7.84 & 7.61-7.54 ppm indicates the presence of *p*-chlorophenylene unit which belongs to 13c,17c,14c and 16c protons of the *p*-chlorophenylene moiety. The protons signals 7-01-6.95 & 7.61-7.54 ppm appeared for 23c & 22c protons of the salicylic acid unit.

Similarly, the compound 3c contains 16 sets of carbons, the ^{13}C NMR spectrum showed the 16 sets of carbon signals. The carbon signal at 172.50 ppm appeared for the carboxylate carbon of thesalicylylunit. The carbon signal at 162.20 ppm appeared for the carbon of hydrazide unit and the peak at 148.21 ppm appeared for imine carbon. The appearance of carbon signals at 150.81 & 122.10 ppm indicates the presence of a pyridinium unit. Similarly, the appearance of carbon signals at 129.01 & 129.47 ppm appeared for the *p*-chlorophenylene unit correspondingly. The carbon signals at 133.46 & 136.11 ppm appeared for 20c & 22c's carbon

which is present in the salicylyl unit. The selected ^{1}H and ^{13}CNMR chemical shiftsof IHCs are represented in **Fig. 2.**

In the FT-IR spectrum, the stretching frequency for hydrazide NH appeared at 3491 cm^{-1}. Similarly, the stretching frequency for the pyridiniumNH unit has appeared at 3396 cm^{-1}. The aromatic ring CH vibrations appeared at 3074 $cm^{-1}$and 3027 cm^{-1} correspondingly. The absorption band at 1738 cm^{-1} appeared for the carbonyl stretching frequency which is present in the hydrazide moiety. The strong absorbance band at 1660 cm^{-1}appeared for C=N stretching vibrations of imine moiety. The band at 1590 cm^{-1} and 1557 cm^{-1}appeared for the C=N unit of pyridinium and C=C unit of aromatic rings. The band at 1216 cm^{-1} appeared for C-O stretching vibrations of carboxylate units. The C-Cl stretching vibration has appeared at 752 cm^{-1} as a strong absorption band.

3.2 Computational study

3.2.1 Frontier molecular orbitals

Highest occupied molecular orbital andlowest unoccupied molecular orbital are used to predict the electrical properties, chemical properties, biological activity, stability and reactivity of thecompounds[29-30].Themolecular orbitals playan important role in calculating the HOMO, LUMO, bandgap and other parameters. In all IHCs, the electron cloud localized as same as each other. In HOMO the electron density is localized in benzoate units and in LUMO the electron density is localized in isoniazid moiety. Comparatively, all the IHCs have more electron density in the region of carboxylate and isoniazid moiety. So the carboxylate and the isoniazid region is a more negative region that could be ready to form the hydrogen bonding interaction with a biomolecule. The same results were obtained in the molecular docking studies since the isoniazid and carboxylate moieties form several hydrogen bonding interactions with the α-

amylase enzyme.The negative energies of HOMO (-5.5670 to -6.0182) and LUMO (-3.2765 to -3.3971) indicate the IHCsare stable molecules.

The bandgap has been used to predict the stability and chemical reactivity of IHCs.The bandgap values of IHCs are in the range of 2.1698 to 4.6474 eV correspondingly. Amid IHCs, the calculated bandgap of compound 3b is higher than others which ismore stable than **3a** and **3c**. The electrophilicity index (ω) is the ability of the molecule to accept the electrons from the environment. Especially, the higher value of electrophilicity index has a higher ability to accept electrons from biomolecules. The results suggested that the compound **3c**exhibitedhigherelectrophilicityindex than others. The calculated electrophilicity index is found to be 9.2581eV which is represented the highest capacity to accept the electrons. Thus the compound 3c has the number of hydrogen bonding interactions in molecular docking studies. Also the other DFT parameters like chemical potential, hardness and softness calculated and presented in **Table 1.**The representation of HOMO and LUMO forIHCs was represented in **Fig. 3, 4**and **5.**

Bandgap $\Delta E = E_{LUMO} - E_{HOMO}$

Chemical potential $\mu = (E_{HOMO} + E_{LUMO})/2$

Global hardness $\eta = (E_{LUMO}-E_{HOMO})/2$

Global softness $\zeta = 1/2\eta$

Electrophilicity index $\omega = \mu^2/2\eta$

3.3 Molecular electrostatic potential

Molecular electrostatic potential was used to identify the bindingregion of a ligand with the biomolecules.In molecular electrostatic potential, the blue color indicates the most positive potential and the red color indicates the most negative potential which willbe very useful for understanding the region responsible for the biological activity of the molecule [31]. Particularly,

the negative potential region of themolecule is more important because it is ready to make hydrogenbonding interaction with protein.In the present research, the molecular electrostatic potential is performed for the synthesized IHCs. The results indicate that the carbonyl present in the molecule showed negative potential. Especially, the carboxylate units displayed the highest negative potential. From these studies, the research is concluded that the carbonyl oxygen and benzoate oxygens are responsible for hydrogen bonding interactions with proteins. The same results obtained in molecular docking studies. Most of the hydrogen bonding interactions formed between the oxygen of IHCs with the α-amylase enzyme. In compound 3c, the negative potential is occupied in many regions which were identified at carbonyl oxygen of hydrazide, carboxylate oxygen and phenolic OH unit. Also, the whole ring of the salicylate unit covered by the negative potential which clearly displays the red colour. Thus the compound 3c showed 5 numbers of hydrogen bonding interactions with theprotein. The hydrogen bonding interactions were identified at carbonyl hydrazide, carboxylate oxygen and phenolic hydroxyl regions respectively.In the case of compounds 3a and 3b, only two hydrogen bonding interactions were identified in the docked complex. The molecular electrostatic potential of IHCs is represented in **Fig. 6.**

3.4 Molecular docking studies

Molecular docking is the most frequently used method which is used to design the structure-based drug, predict the binding conformation of small molecules to the applicable target binding site and to develop the new drug candidate[31].α-amylase is a key enzyme in the digestive system and catalyzes the initial step in starch hydrolysis.Its inhibitors possess an important role in controlling diabetes. Hence the research is decided to choose theα-amylase enzymes for the molecular docking studies[32].

The obtained docking results indicated that compound**3c**exhibited strong interaction with the α-amylase enzyme.The compound **3a** showed two hydrogen bonding interactions with ARG421 and SER3. The binding energy of 3a is found to be -294.42 KJ/mol. The compound **3b**formedtwo hydrogen bondinginteractions withTYR2 and SER3 amino acid with good binding energy. Similarly, the compound **3c** showed five hydrogen bonding interactions with THR377, TRP388, ARG389, GLN390 andLYS322amino acids with good binding energy. The calculated binding energies of **3b** and **3c** are found to be -315.24 and -299.78 KJ/mol respectively. In the docked complex of **3a**, the chlorine forms a hydrogen bonding interaction with quinidine NH of ARG421. Similarly, the carboxylate oxygen forms a hydrogen bonding interaction with OH of SER3.

In the docked complex of **3b**, the carbonyl of hydrazide forms the hydrogen bonding interaction with CH of SER3 and NH of TYR2. In the case of **3c**, the imine nitrogen forms a hydrogen bonding interaction with guanidine NH of ARG389 and NH of GLN390. The hydrazide carbonyl forms a hydrogen bonding interaction with NH of GLN390 and NH of LYS322. Similarly, the carboxylate oxygen forms a hydrogen bonding interaction with indole NH of TRP388. The OH of **3c** forms hydrogen bonding interaction with NH of THR377.

Based on the docking results, the research is concluded that the IHCsare good anti-diabetic active compounds.The various binding interactions of IHCs with α-amylaseare represented in **Fig.7** and binding energy, thenumber of hydrogen bonding interactions are represented in **Table 2.**

3.5 Biological Evaluation

3.5.1 BSA denaturation technique

The original structure of the protein destroys by the external stress in the protein denaturation process. And also it takes place from the chemical processes or interaction of compounds such as base or strong acid, a concentrated inorganic salt, organic solvent or heat. The denaturation of proteins is the cause of losing their biological function which leads to inflammation. As part of the research on the mechanism of the anti-inflammation activity, the ability of IHCs to inhibit protein denaturation was studied using the bovine serum albumin (BSA) denaturation technique.Percentage inhibition for the screened compounds was determined and compared withdiclofenac sodium which is used as a reference drug.Various concentrations of IHCs and standard drugs are prepared and tested for their anti-inflammatory using bovine serum albumin. The percentage inhibition of compound **3b** is in the range of 25.7 to 82.4%.Similarly, the compound **3c** exhibited anti-inflammatory activity in the range of 27.2 to 80.2%. The compound **3b** and **3c** showed better/nearer activity to standard drugs.The **3c**compound is slightly less active than that of its standard.

Another protein denaturation activity was performed using egg albumin. All the IHCs showed very good anti-inflammatory activity in the egg albumin denaturation method. In the case of egg albumin denaturation, the compound **3a** showed potent activity than others. The egg albumin denaturation activities are in the order of **3a>3b>3c**. The percentage inhibition of Bovine serum albumin and Egg albumin denaturation was represented in **Fig.8a** and **8b**. The anti-inflammatory activity results clearly showed that the IHCs showed very good activity against both bovine serum and egg albumin proteins which is nearer to standard diclofenac sodium. All the IHCs showed similar activity and the negligible variation was identified in the percentage inhibitions of IHCs. The hydrazones have been proved as very good anti-inflammatory agents that could be the reason the potent activity of IHCs.[33-35]

3.6 Antidiabetic activity

3.6.1*α*-amylase inhibitory activity

The pancreatic α-amylaseplays a significant rolein the digestion of carbohydrates/starch which breaks down the starch/carbohydrates to small glucose units. The inhibition of α-amylase can lead to the reduction of postprandial hyperglycemia in diabetic conditions. TheIHCs were tested their α-amylase inhibitory activity by the dinitrosalicylic acid (DNSA) method followed by Al-Zuhair *et al* [24]. Concentrations versus % inhibition curves were plotted for theIHCs and standard. Acarbose is used as the standard drug. The percentage inhibition was tested at different concentrationslike 10,50, 100, 250 and 500 µg/mL respectively.The results revealed that theIHCs displayed agood activity with better% inhibitions. The inhibitions are nearer tostandardacarbose and the IHCs show similar α-amylase inhibitory activity. The IHCs and acarbose's antidiabetic activity against α-amylase is represented in **Fig. 9.**

4. Conclusion

The designed IHCs were successfully synthesized and well characterized by standard spectroscopic techniques.The structure of the IHCs was very clearly interpreted and discussed.The IHCs showed very goodanti-inflammatory and their percentage inhibition was nearer to standard. Similarly, the IHCs showed very good α-amylase inhibitory activity.The IHCs exhibited good binding energy and binding interactions with theα-amylase enzyme. The compound **3b** showed thehighest binding energy of -315.83 and compound **3c** forms 5 numbers of hydrogen bonding interaction with 1HNY.The more number of hydrogen bonding interactions of IHCs-1HNY complexes conclude that the IHCs are very good antidiabetic agents.The calculated parameters HOMO and LUMO using DFT calculations clearly supported the docking

interactions. The bandgap of IHCs was less it concludes that the IHCs are more reactive complexes that could be the reason for the highest biological activity.

Acknowledgment

The authors grateful toBiochemie Innovations Lab, Tindivanam-604001 for consultancy service during this research work.

Figures and captions

Fig. 1: Designed complexes of Isoniazid-hydrazone complexes (IHCs).

Fig. 2: Selected ^{1}H NMR and ^{13}C NMR chemical shifts of IHCs

Fig. 3. Frontier molecular orbital of 3a.

Fig. 4. Frontier molecular orbital of 3b

Fig. 5. Frontier molecular orbital of 3c

Fig. 6. Molecular electrostatic potential of IHCs.

Fig. 7: Binding interaction of IHCs with 1HNY.

Fig. 8 (a) Anti-inflammatory activity (BSA denaturation method) ofIHCs **(b)** Anti-inflammatory activities (Egg albumin denaturation method) ofIHCs.

Fig. 9. Anti-diabetic activityofIHCs.

Scheme 1. Synthetic route for IHCs.

Tables and captions

Table 1: DFT calculations of IHCs.

Table 2: Molecular docking interaction of IHCsagainst α-amylase.

References and Notes

1. E. Grunberg, R. J. Schnitzer, Proc. SOC, Exp. Biol. Med. 84 (1953) 220.
2. M. V. N. De Souza, Current Status and future prospects for new therapies for pulmonary tuberculosis. Curr.Opin.Pulm. Med. 12(2006) 167–171.
3. B. Lei, C-J. Wei, S.C.Tu, Action mechanism of antitubercular isoniazid activationby Mycobacterium tuberculosis KatG, isolation, and characterization of InhA inhibitor. J. Biol. Chem. 275 (2000) 2520-2526.
4. S.Karthikeyan, M. S.Krishnmoorthy, Effect of subacute administration of isoniazidand pyridoxine on lipids in plasma, liver and adipose tissues in the rabit.Drug Chem.Toxicol. 14 (1991) 293-303.
5. H. K. Jahromi, M. Pourahmad, H. A. Abedi, M. karimi, Z. K.Jahromi, Protective effects of salep against isoniazid liver toxicity in wistar rats, J.Tradit. Complement Med, 8 (2018)239–243.
6. S.Rollas, N.Gulerman, H.Edeniz, Synthesis and Antimicrobial Activity of Acid Hydrazide and 3-Acetyl-2,5-Dis- ubstituted-1,3,4-Oxadiazolines. Farmaco. 57(2002) 171-174.
7. J. R.Dimmock, S. C Vasishtha, J. P. Stables, Anticonvulsant properties of various acetylhydrazones, aromaticand unsaturated carbonyl compounds, Eur. J. Med. Chem. 35(2000) 241-248.
8. P. C. Lima, L. M. Lima, K. C. Silva, P. H. Leda, A. L. P Miranda, C.A.M.Fraga, E. J. Barreiro, Synthesis andanalgesic activity of novel-acylarylhydrazones and isosters, derived from natural safrole, Eur. J. Med.Chem. 35 (2000) 187-203.

9. U.Salgin-Goksen, N. Gokham-Keleci, O.Gostal, Y.Koysal, E.Kilici, S.Isik, G.Aktay, M.Ozalp, 1-Acylthiosemicarbazides, 1,2,4-triazole-5(4H)-thiones, 1,3,4-thiadiazoles and hydrazones containing 5-methyl-2-benzoxazolinones: Synthesis, analgesic-anti-inflammatory and antimicrobial activities. Bioorg.Med. Chem. 15(2007) 5738-5751.
10. A.Imramovsky, S.Polanc, J. Vinsova, M.Kocevar, J.Jampitek, Z.Reckova, J. A Kaustova. A newmodification of anti-tubercular active molecules. Bioorg. Med. Chem. 15(2007) 2513-2551.
11. S. A. M. El-Hawash, W. A. E Abdel, M. A. El-Dewellawy. Synthesis of Some New Quinoxalines and 1,2,4-Triazolo[4,3-a]-quinoxalines for Evaluation of in vitro Antitumor and Antimicrobial Activities, Arch.Pharm. Chem. Life Sci. 339(2006) 564-571.
12. P.T.Peter, S.Sah,AndersonPeoples, IsonicotinylHydrazones as Antitubercular Agents and Derivatives for Identification of Aldehydes and Ketones,J. Am. Pharm. Assoc.43(1954) 513-524.
13. M. J. Hearn and M. H. Cynamon,Design and synthesis of antituberculars: preparation and evaluation against *Mycobacterium tuberculosis* of an isoniazid Schiff base,J. Antimicrobial Chemother. 53(2004) 185–191.
14. J. Lehar, A. S Krueger, W. Avery, A. M.Heilbut, L. M. Johansen, Synergistic drug combinations tend to improve therapeutically relevant selectivity, Nat.Biotechnol. 27 (2009) 659–666.
15. T. Stanton, J. L. Reid,Fixed dose combination therapy in the treatment ofhypertension. J.Hum.Hypertens. 16, (2002) 75–78.

16. S. U.Bokhari, U. M. Gopal, W. C. Duckworth, Beneficial effects of aglyburide/metformin combination preparation in type 2 diabetes mellitus.Am. J.Med.Sci. 325 (2003) 66–69.
17. X. M. Zhao, M. Iskar, G. Zeller, M. Kuhn, V. vanNoort, P. Bork,Prediction of Drug Combinations by Integrating Molecular and PharmacologicalData.PLoSComput.Biol. 7 (2011) e1002323.
18. M.M. Amiji, T. J. Cook, W. Cary Mobley, Complexation and Protein Binding, Book Chapter, Applied Physical Pharmacy. 2e.
19. P. M.Soares, M. C. A.Patrocı´nio, A. S. Assreuy, R. C. L. Siqueira, N. M. Lima , M.O.V. Arrud , S. S. Escudeiro , K. M. de Carvalhoa, F. C. F.Sousa, G. S. BarrosVian, S. M. M. Vasconcelos, Aminophylline (a theophylline–ethylenediamine complex) blocks ethanol behavioral effects in mice, Behav. Pharmacol.20 (2009) 297–302.
20. V. B. Chaudhary, J. K. Patel, Cyclodextrin inclusion complex to enhance solubility of poorly water soluble drugs: a review, Int. J. Pharm. Sci. Res. 4 (2013)68-76.
21. A. Lavanya, R. Sribalan, V. Padmini, Synthesis and biological evaluation of new benzofurancarboxamide derivatives, J. Saudi Chem. Soc. 27(2017) 277-285.
22. G. Banuppriya, R. Sribalan, V. Padmini, Synthesis and characterization of curcumin-sulfonamide hybrids: Biological evaluation and molecular docking studies, J. Mol. Struct. 1155(2018) 90-100.
23. A. Lavanya, R. Sribalan, V. Padmini, Synthesis and Biological evaluation of benzofurancarboxamide derivatives, J. Saudi Chem. Soc. 21(2017) 277-285.

24. S. Al-Zuhair, A. Dowaidar, H. Kamal, 'Inhibitory Effect of Dates-extract on a-amylase and b-glucosidase Enzymes Relevant to Non-insulin Dependent Diabetes Mellitus', J. Biochem. Technol. 2(2010) 158 – 160.
25. S.M.D. Rizvi, S. Shakil, M. Haneef, A simple click by click protocol to perform docking: autodock 4.2 made easy for non-bioinformaticians, Excli J. 12 (2013) 831-857.
26. Y.Y. Xu, Y. Cao, H. Ma, H.Q. Li, G.Z. Ao, Design, synthesis and molecular docking of α,β-unsaturated cyclohexanone analogous of curcumin as potent EGFR inhibitors with antiproliferative activity, Bioorg. Med. Chem. 21 (2013) 388-394.
27. G.D. Brayer, Y.Luo, S. G. Withers, The structure of human pancreatic α-amylase at 1.8 Å resolution and comparisons with related enzymes, Protein Sci. 4 (1995) 1730-1742.
28. M.J. Frisch, G.W. Trucks, H.B. Schlegel, G.E. Scuseria, M.A. Robb, J.R. Cheeseman, J.A. Montgomery Jr., T. Vreven, K.N. Kudin, J.C. Burant, J.M. Millam, S.S. Iyengar, J. Tomasi, V. Barone, B. Mennucci, M. Cossi, G. Scalmani, N. Rega, G.A. Petersson, H. Nakatsuji, M. Hada, M. Ehara, K. Toyota, R. Fukuda, J. Hasegawa, M. Ishida, T. Nakajima, Y. Honda, O. Kitao, H. Nakai, M. Klene, X. Li, J.E. Knox, H.P. Hratchian, J.B. Cross, V. Bakken, C. Adamo, J. Jaramillo, R. Gomperts, R.E. Stratmann, O. Yazyev, A.J. Austin, R. Cammi, C. Pomelli, J.W. Ochterski, P.Y. Ayala, K. Morokuma, A. Voth, P. Salvador, J.J. Dannenberg, V.G. Zakrzewski, S. Dapprich, A.D. Daniels, M.C. Strain, O. Farkas, D.K. Malick, A.D. Rabuck, K. Raghavachari, J.B. Foresman, J.V. Ortiz, Q. Cui, A.G. Baboul, S. Clifford, J. Cioslowski, S.B.B. tefanov, G. Liu, A. Liashenko, P. Piskorz, I. Komaromi, R.L. Martin, D.J. Fox, T. Keith, M.A. AlLaham, C.Y. Peng, A. Nanayakkara, M. Challacombe, P.M.W. Gill, B. Johnson, W. Chen, M.W. Wong, C.

Gonzalez, J.A. Pople, Gaussian 03, Revision C.02, Gaussian, Inc., Wallingford, CT, 2004.

29. K. Sarojinidevi, P. Subramani, M. Jeeva, N. Sundaraganesan, M. S. Boobalan, G. V. Prabhu, Synthesis, molecular structure, quantum chemical analysis, spectroscopic and molecular docking studies of N-(Morpholinomethyl) succinimide using DFT method, J. Mol. Struct. 1175 (2018) 609-623.
30. P. Shafieyoon, E. Mehdipour, Y. S.Mary, Synthesis, characterization and Biological Investigation of glycine- based sulfonamide derivative and its complex: vibration assignment, HOMO–LUMO analysis, MEP and molecular docking, J. Mol. Struct.1181, (2019) 244-252.
31. K.P. SafnaHussan, M. ShahinThayyil, Vijisha K.Rajan, K. Muraleedharan, DFT studies on global parameters, antioxidantmechanism and molecular docking of amlodipine besylate,80, 2019, 46-53.
32. G.Banuppriya, R. Sribalan, S. A. R. Fathima, V.Padmini,Synthesis of β-Ketoamide Curcumin Analogs for Anti-Diabetic andAGEs Inhibitory Activities,Chem. Biodivers.15(2018) 1800105.
33. C. M. Moldovan, O. Oniga, A. Parvu, B. Tiperciuc, P. Veritec, A. Pirnau, O. Crisan, M. Bojita, R. Pop, Synthesis and anti-inflammatory evaluation of some new acyl-hydrazones bearing 2-aryl-thiazole, Eur. J. Med. Chem. 46 (2011) 526-534.
34. S. M. Sondhi, M. Dinodia, A. Kumar, Synthesis, anti-inflammatory and analgesic activity evaluation of some amidine and hydrazone derivatives, Bioorg. Med. Chem. 14 (2006) 4657-4663.

35. U. Salgm-Goksen, N. Gokhan-kelekci, O. Goktas, Y. Koysal, E. Kilic, S. Isik, G. Aktay, M. Ozalp, Bioorg. Med. Chem, 15 (2007) 5738-5751.